Moulding flexural waves in elastic plates lying atop a Faqir's bed of nails

T. Antonakakis[1,2], R. V. Craster [2], S. Guenneau[3]
[1] *European Organization for Nuclear Research, CERN CH-1211, Geneva 23, Switzerland*
[2] *Department of Mathematics, Imperial College London, London SW7 2AZ, UK and*
[3] *Institut Fresnel, UMR CNRS 6133, University of Aix−Marseille, Marseille, France*

Platonic crystals (PCs) are the elastic plate analogue of the photonic crystals widely used in optics, and are thin structured elastic plates along which flexural waves cannot propagate within certain stop band frequency intervals. The practical importance of PCs is twofold: these can be used either in the design of microstructured acoustic metamaterials or as an approximate model for surface elastic waves propagating in meter scale seismic metamaterials. Here, we make use of the band spectrum of PCs created with very small clamped holes, the nails of the title, to achieve surface wave reflectors at very large wavelengths, a flat lens, an endoscope, a directive antenna near stop band frequencies and cloaking from Dirac cones. The point pinned, Faqir, plate is particularly appealing as there is an exact dispersion relation available so the origin of these phenomena can be explained and interpreted using Fourier series and high frequency homogenization.

There has been much interest over the past 20 years in the analysis of elastic waves in thin plates in the continuum mechanics community [1, 5, 19, 24, 26, 27, 29]; an interest renewed in the metamaterial community with the theoretical proposals [4, 13–15], and their subsequent experimental validation [6, 32, 33], of broadband cloaks and negatively refracting flat lenses for flexural waves.

One of the attractions of platonics is that much of the physics of photonic crystals can be translated into platonic crystals (PCs). There are mathematical subtleties in the analysis, and numerics, of the scattering of flexural waves [29] owing to the fourth-order derivatives, versus the usual second-order derivatives for the wave equation of optics, involved in the governing equations; even the waves within a perfect plate have differences from those of the wave equation as they are not dispersionless.

There is a long history of wave propagation along periodically supported plates motivated by ribbed structures in underwater acoustics, [25]; the periodically pinned plate [24] being considered in detail. Movchan et al. [26] also give a complementary treatment for the flexural plate with doubly periodic domains of circular holes using lattice sums and multipoles with a dilute limit giving approximate dispersion relations in closed form. Fourier series expansions introduced in [12, 24] and applied in [5] also allow for a highly accurate analytic expression for the exact dispersion equation for pinned plates. We follow this latter route, which combined with the recently developed high frequency homogenization theory (HFH) [11], uncovers the physics of pinned Faqir [34] plates; a striking illustration (lensing via all-angle-negative refraction) is shown in Fig. 1(a), which contrasts with a shielding effect at a lower frequency in Fig. 1(b). The latter obviously has potential application in seismic metamaterials [8] for anti-earthquake systems.

Much has been said about control of light [31], sound, water, or shear (SH) waves [9] using the rich behaviour encapsulated by the dispersion curves of bi-periodic structures, modelled by a Helmholtz equation, up to minor changes in the normalization of material parameters, and choice of boundary conditions (e.g. Dirichlet or Neumann for clamped or freely vibrating inclusions in the context of SH waves). However, when one moves into the area of elastic waves, governed by Navier equations, it is no longer possible to reduce the analysis to a sin-

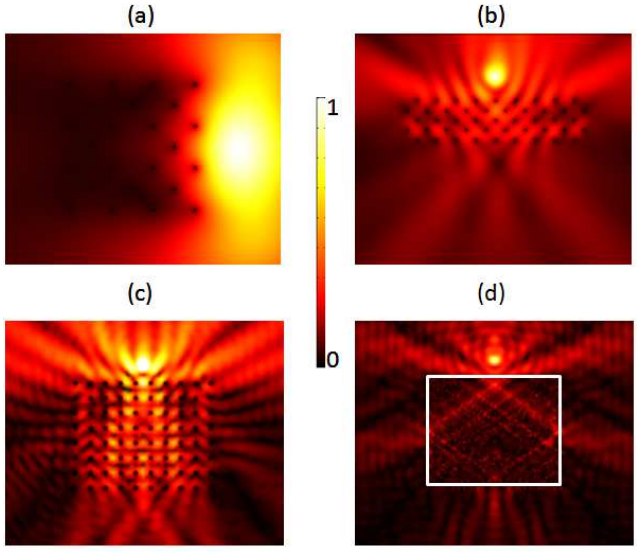

Figure 1: (a) A forcing generates a bending wave totally reflected by the array (with 22 clamped holes), throughout the zero-frequency stop band of Fig. 2 (here $\Omega = 2$). From the four-fold symmetry of the array and linearity of Eq.1, the defect at the center of the array (one missing hole) is shielded from bending waves generated by a forcing. (b) A bending wave excited by a point forcing of normalized frequency $\Omega = 2.6$ is focused through an array (pitch 2) of 27 clamped holes (radius 0.01) tilted through an angle $\pi/4$. (c) Focusing through an array of 304 clamped holes of radius 0.01 in a regular square orientation at the same frequency of $\Omega = 2.6$. (d) Represents the focusing effects produced by an effective material governed by equation (6) with $T_{11}T_{22} \leq 0$ yielding characteristic type of solutions.

gle scalar partial differential equation (PDE), as shear and pressure waves do couple at boundaries. There is nevertheless, the simplified framework of the Kirchhoff-Love plate theory [16] that allows for bending moments and transverse shear forces to be taken into account via a fourth-order PDE for the out-of-plane plate displacement field. This plate theory is a natural extension of the Helmholtz equation to a generic model for flexural wave propagation through any spatially varying thin elastic medium. It offers a very convenient mathematical model for any physicist wishing to grasp (some of) the physics of PCs using earlier knowledge in photonic or phononic crystals. However, while the Helmholtz equation can, with appropriate notational and linguistic changes, hold for acoustic, electromagnetic, water or out-of-plane elastic waves and so encompasses many possible applications, the Kirchhoff-Love plate theory is dedicated to the analysis of flexural waves. For instance, it says little about propagation of in-plane elastic waves in platonic crystals.

Bearing this restriction in mind, we solve

$$\left(\frac{\partial^2}{\partial x_1^2}+\frac{\partial^2}{\partial x_2^2}+\Omega\right)\left(\frac{\partial^2}{\partial x_1^2}+\frac{\partial^2}{\partial x_2^2}-\Omega\right)u=0, \qquad (1)$$

[16, 22] for $u(x_1,x_2)$ on the square cell $-1<x_1,x_2<1$. Here, $\Omega^2=12(1-\nu^2)\rho\omega^2/(Eh^2)$, where ρ, h, E, ν are density, thickness, Young's modulus and Poisson's ratio of the plate, respectively, and ω is the angular wave frequency; the plate contains an array of very small inclusions, with Dirichlet (clamped) boundary conditions, which is a good model for rigid nails of the Faqir plate.

In the context of optics, (1) reduces to a second order PDE where only the first factor of (1) appears, in which case Dirichlet boundary conditions are a good model for infinite conducting thin wires at GHz frequencies, with the unknown u of such a Helmholtz equation being the longitudinal component of the electric field E_z in TM polarization and the spectral parameter Ω is associated with $\omega^2\varepsilon(x_1,x_2)/c^2$ whereby ω is the electromagnetic wave frequency, ε is the relative permittivity and c is the speed of light in a vacuum. Such a model has been known since the mid 90s to lead to a zero frequency stop band associated with very low frequency plasmons [28, 30].

For waves propagating through an infinite, perfect, doubly periodic medium, one can invoke Bloch's theorem [7, 21] and simply consider a square cell with quasi-periodic conditions applied to the edges:

$$u(1,x_2)=e^{2\mathrm{i}\kappa_1}u(-1,x_2), \quad u_{x_1}(1,x_2)=e^{2\mathrm{i}\kappa_1}u_{x_1}(-1,x_2), \qquad (2)$$

$$u(x_1,1)=e^{2\mathrm{i}\kappa_2}u(x_1,-1), \quad u_{x_2}(x_1,1)=e^{2\mathrm{i}\kappa_2}u_{x_2}(x_1,-1), \qquad (3)$$

with the Bloch wave-vector $\boldsymbol{\kappa}=(\kappa_1,\kappa_2)$ characterizing the phase-shift going from one cell to the next. Also $u=0$ at the origin with continuity of u,u_{x_1},u_{x_2} there also. The exact solution is readily found [5, 24] as

$$u(\mathbf{x})=\exp(i\boldsymbol{\kappa}\cdot\mathbf{x})\sum_{n_1,n_2}\frac{\exp(-i\pi\mathbf{N}\cdot\mathbf{x})}{[(\kappa_1-\pi n_1)^2+(\kappa_2-\pi n_2)^2]^2-\Omega^2}, \qquad (4)$$

and enforcing the condition at the origin gives the dispersion relation $D(\boldsymbol{\kappa},\Omega)=0$ where

$$D(\boldsymbol{\kappa},\Omega)=\sum_{n_1,n_2}\frac{1}{[(\pi n_1-\kappa_1)^2+(\pi n_2-\kappa_2)^2]^2-\Omega^2}. \qquad (5)$$

As is well-known in solid state physics [7] only a limited range of wavenumbers need normally be considered, namely the wavenumbers along the right-angled triangle ΓXM shown in the irreducible Brillouin zone inset in Fig. 2. There are however some exceptions, where it is possible to miss important details such as the stop band minima/maxima not occuring at the edges of the Brillouin zone [2, 3, 18] and flat bands leading to strong anisotropy and slow light [10].

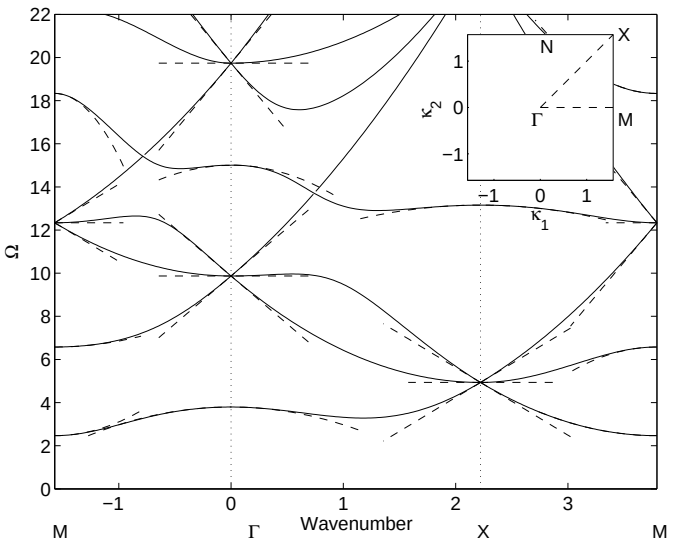

Figure 2: Bloch dispersion curves around the edges of the Brillouin zone ΓXM (inset) for an array of clamped holes (radius 0.01) of pitch 2. One notes the stop band for $\Omega\in[0,\pi^2/4]$ and three Dirac cones at frequencies $\Omega=\pi^2/2$ (X point), π^2 and $2\pi^2$ (Γ point). Solid curves are computed with FEM, and dashed curves are from HFH.

The dispersion diagram is shown in Fig. 2; the singularities of the summand in Eq. (5) correspond to solutions within a square cell (without the nail) satisfying the Bloch conditions at the edges, in some cases these singular solutions also satisfy the conditions at the support and are therefore true solutions to the problem. Solid lines in Fig. 2 are the dispersion curves double checked by the finite element method (FEM) using the commercial package Comsol, notable features are the zero-frequency stop-band and also crossings of branches at the edges

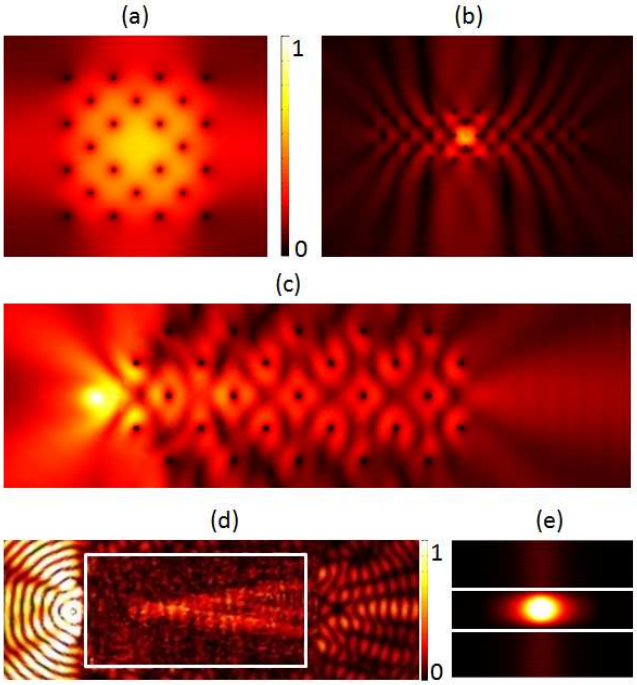

Figure 3: A bending wave excited by a forcing of normalized frequency $\Omega = 3.7952$ (that of vanishing group velocity at Γ point in Fig. 2) inside an array of pinned holes (pitch 2, radius 0.01) tilted through an angle $\pi/4$ gives rise to respectively four (a) and two (b) highly-directed beams outside 24 holes making a square (a) and 27 holes making a rectangle (b). When tilted through an angle $\pi/4$ (c) the same array with 27 holes acts has an endoscope for a source at frequency $\Omega = 2.4674$. The endoscope (d) and antenna (e) effects are simulations of the continuum PDEs (6) generated by HFH with respective (T_{11}, T_{22}) coefficients of $(-9.649, 4.7149)$ at point M and $(6.2524, 6.2524)$ at point Γ, where the effective media are highlighted by white lines.

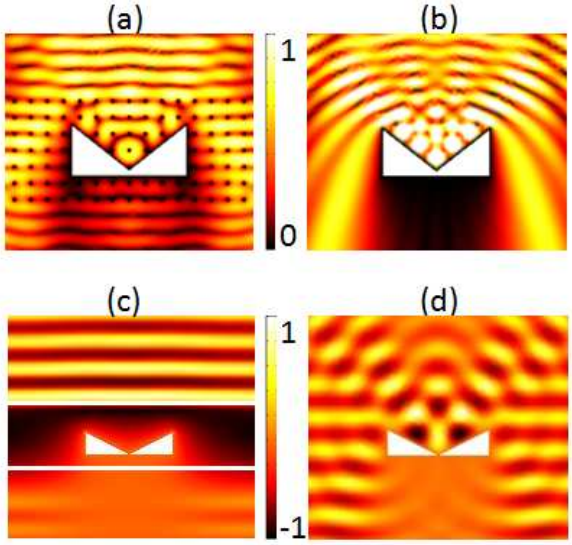

Figure 4: A plane bending wave of normalized frequency $\Omega = 9.7$ (just below the first Dirac cone at Γ point in Fig. 2) incident from the top on an array of pinned holes (pitch 2, radius 0.01) undergoes considerably less scattering (a) than by a clamped obstacle on its own (b). Again the asmptotic PDEs in equation (9) capture the essence of physics of cloaking (c) and scattering (d) by the same clamped obstacle.

of the Brillouin zone. Importantly, HFH [5] captures the physics of this band diagram, with the asymptotic theory giving dashed curves that fit very well with the FEM (solid curves) near the band-gap edges which are the zero-group velocity and Dirac points. The multiple scales used for HFH are a short-scale $\xi_i = x_i/l$ and a long-scale $X_i = x_i/L$ for $i = 1, 2$ where l and L represent respectively the characteristic small scale (half length of a cell) and the long scale. A small parameter is formed as $\epsilon = l/L$ and an expansion of $\Omega^2 = \Omega_0^2 + \epsilon\Omega_1^2 + \dots$ and $u = u_0 + \epsilon u_1 + \dots$ is posed with respect to this parameter. It turns out that the leading order term for u is $u_0(\boldsymbol{\xi}, \mathbf{X}) = f_0(\mathbf{X})U_0(\boldsymbol{\xi})$ where the function f_0 representing an envelope of the solution u is obtained by an equation only on the long scale as,

$$T_{ij} f_{0,X_i X_j} - \Omega_2^2 f_0 = 0. \tag{6}$$

where T_{ij}'s are integrated quantities of the leading order and first order short scale solutions with $T_{ij} = 0$ for $i \neq j$ in the present illustrations and Ω_2 is simply the second order term of the Ω expansion. As in [5], assuming Bloch waves, the asymptotic dispersion relation for Ω reads,

$$\Omega \sim \Omega_0 - \frac{T_{ij}}{2\Omega_0}\kappa_i\kappa_j, \tag{7}$$

where $\kappa_i = K_i - d_i$ and $d_i = 0, -\pi/2, \pi/2$ depending on the location in the Brillouin zone about which the asymptotic expansion originates, and Ω_0 is the standing wave frequency at the Brillouin zone edge ; these asymptotics give the dashed curves in Fig. 2. For the case of multiple modes originating from the same point, as for example the Dirac points, Eq. (7) is no longer valid and one obtains three coupled equations for $f_0^{(i)}$ that simplify to three similar anisotropic equations like (6). Note that Eq. (6) is of second order and not fourth. The fourth order plate equation yields two types of solutions namely propagating and exponentially decaying. Indeed in the long scale, solutions follow a second order PDE and the remaining information of the fourth order problem is enclosed in the T_{ij} integrated quantities.

We give three potential applications of the platonic crystal described by fig. 2, on top of the slab lens shown in fig. 1 as well as comparison solutions constructed from the continuum long-scale HFH theory; the coefficients T_{ij} capture the potential strong anisotropy of the medium.

Using the vanishing group velocity of the second dispersion curve in fig. 2 in the neighborhood of the Γ point,

one can design a strongly directive antenna, as shown in fig. 3(a,b) and (e). The effective medium for the directive antennas is governed by Eq. (6) with $T_{11} = T_{22} = 6.2524$. In Fig. 3(e) the group velocity is calculated by differentiating Eq. (7) with respect to κ_1 to obtain,

$$\Omega_{,\kappa_1} \sim -\frac{T_{11}}{\Omega_0}\kappa_1, \tag{8}$$

and similarly for κ_2.

Fig. 3(c) and (d) shows an endoscope effect wherein a point source located close to a tilted array leads to focussing and a strong localised beam. The behaviour near point M of the Brillouin zone is responsible for the focussing effects of Fig. 1 and Fig. 3(c). Here the closest standing wave frequency is at the point M and unequal T_{ii} coefficients that have opposite signs. This leads to very strong anisotropy within the effective material directed along characteristics; the effective material becomes hyperbolic rather than elliptic. By considering only a portion of the Brillouin zone we must bear in mind that this asymptotic solution is also valid at N and there is a second f equation with the T_{11} and T_{22} interchanged that is used. The asymptotic PDE for HFH is Eq. (6) with $T_{11} = -9.649$ and $T_{22} = 4.7149$. Ω_2 is determined using the the frequencies stated in Figs 1 and 3(c) with Eq. (7). The opposite sign of coefficients T_{11} and T_{22} yield characteristic type of solutions in order to obtain an endoscope effect.

Last, but not least, the triple crossings in the dispersion diagram Fig. 2 comprise Dirac cones with a flat mode passing through the vertex. This is highly interesting given that Dirac cones are normally limited to graphene-like hexagonal structures [17]; the current situation involves a square lattice is akin to the Dirac cones for photonic crystals recently described in [20, 23]. One can use the properties of Dirac cones to reduce the scattering of a clamped obstacle in a pinned PC, as demonstrated in fig. 4(a),(b). This behaviour is also captured by HFH asymptotics: In this particular case three coupled equations emerge with variables $f_0^{(i)}$ for $i = 1, 2, 3$. The system decouples to yield the same governing equation for all three functions $f_0^{(i)}$ as,

$$8\pi^6 f_{0,X_iX_i} - \Omega_1^2 f_0 = 0, \tag{9}$$

where Ω_1 is now the first order correction term for the frequency [5]. The numerics using HFH are also shown in Fig. 4(c).

In conclusion, a simplified model of elasticity via the thin-plate equation allows for analytical and numerical studies opening interesting possibilities in the design of flat lens, directive antenna, endoscope, shielding and a cloak for flexural waves. Moreover, such designs could be scaled up in order to achieve some control of seismic surface waves [8], [**?**], indeed this work is motivated by a requirement at CERN to control elastic waves created by thermal shock. We also show, for the first time, that the computations using the recently developed HFH are capable of capturing the fundamental wave propagation features of these various possibilities, including counter-intuitive physics of Dirac points [23].

[1] Abrahams, I. D., and A. N. Norris (2000), Proc. R. Soc. Lond. A **456**, 1559.

[2] Adams, S. D. M., R. V. Craster, and S. Guenneau (2008), Proc. R. Soc. Lond. A **464**, 2669.

[3] Adams, S. D. M., R. V. Craster, and S. Guenneau (2009), Waves in Random and Complex Media **19**, 321.

[4] Al-Lethawe, M. A., M. Addouche, A. Khelif, and S. Guenneau (2012), New J. Phys. **14**, 123030.

[5] Antonakakis, T., and R. V. Craster (2012), Proc. R. Soc. Lond. A **468**, 1408.

[6] Bonello, B., L. L. Belliard, J. Pierre, J. O. Vasseur, B. Perrin, and O. Boyko (2010), Phys. Rev. B **82**, 104109.

[7] Brillouin, L. (1953), *Wave propagation in periodic structures: electric filters and crystal lattices*, 2nd ed. (Dover, New York).

[8] Brule, S., E. Javelaud, S. Guenneau, S. Enoch, and D. Komatitsch (2012), in Proceedings ETOPIM 9 (Marseille, September 2-7), Ed. S. Enoch and S. Guenneau .

[9] Craster, R., and S. Guenneau (2012), *Acoustic metamaterials: Negative refraction, imaging, lensing and cloaking* (Springer Verlag, London).

[10] Craster, R. V., T. Antonakakis, M. Makwana, and S. Guenneau (2012), Phys. Rev. B **86**, 115130.

[11] Craster, R. V., J. Kaplunov, and A. V. Pichugin (2010), Proc R Soc Lond A **466**, 2341.

[12] Evans, D. V., and R. Porter (2007), J. Engng. Math. **58**, 317.

[13] Farhat, M., S. Guenneau, and S. Enoch (2009), Phys. Rev. Lett. **103**, 024301.

[14] Farhat, M., S. Guenneau, and S. Enoch (2010), European Physics Letters **91**, 54003.

[15] Farhat, M., S. Guenneau, S. Enoch, A. Movchan, and G. Petursson (2010), Appl. Phys. Lett. **96**, 081909.

[16] Graff, K. F. (1975), *Wave motion in elastic solids* (Oxford University Press).

[17] H., A. H. C. N., F. Guinea, N. M. R. Peres, K. S. Novoselov, and A. K. Geim (2009), Rev. Modern Phys. **81**, 109.

[18] Harrison, J. M., P. Kuchment, A. Sobolev, and B. Winn (2007), J. Phys. A - Math **40**, 7597.

[19] Howe, M. S. (1994), Proc. R. Soc. Lond. A **444**, 555.

[20] Huang, X., Y. Lai, Z. H. Hang, H. Zheng, and C. T. Chan (2011), NATURE MATERIALS **10**, 582.

[21] Kittel, C. (1996), *Introduction to solid state physics*, 7th ed. (John Wiley & Sons, New York).

[22] Landau, L. D., and E. M. Lifshitz (1970), *Theory of elasticity*, 2nd ed. (Pergamon Press).

[23] Liu, F., Y. Lai, X. Huang, and C. T. Chan (2011), Phys. Rev. B **84**, 224113.

[24] Mace, B. R. (1996), J. Sound Vib. **192**, 629.

[25] Mead, D. J. (1996), J. Sound Vib. **190**, 495.

[26] Movchan, A. B., N. V. Movchan, and R. C. McPhedran

(2007), Proc. R. Soc. Lond. A **463**, 2505.
[27] Murphy, J. E., and G. Li (1994), J. Acoust. Soc. Am. **96**, 2313.
[28] Nicorovici, N. A., R. C. McPhedran, and L. C. Botten (1995), Phys. Rev. Lett. **75**, 1507.
[29] Norris, A. N., and G. R. Wickham (1995), Proc. R. Soc. Lond. A **451**, 631.
[30] Pendry, J. B., A. J. Holden, D. J. Robbins, and W. J. Stewart (1996), Phys. Rev. Lett. **76**, 4773, doi:10.1103/PhysRevLett.76.4773.
[31] Ramakrishna, S. A. (2005), Rep. Prog. Phys. **68**, 449.
[32] Stenger, N., M. Wilhelm, and M. Wegener (2012), Phys. Rev. Lett. **108**, 014301.
[33] Veres, I. A., T. Berer, O. Matsuda, and P. Burgholzer (2012), J. Appl. Phys. **112**, 053504.
[34] The well-known circus trick, or physics demonstration, of a person lying atop a bed of nails being traditionally attributed to travelling Faqirs